Synthesis of Iron oxide Nanoparticle using Propolis from Northern Cyprus and Evaluation of its Antibacterial, Anticancer Potential on MDA-MB 231 cells

[1,3]Sunday Onyebuchi Ukanwa* and [2,3]Erkay Özgör
[1]*Department of Bioengineering, Faculty of Engineering, Cyprus International University, Nicosia, North Cyprus, Mersin 10, Turkey.*
[2]*Department of Molecular Biology and Genetics, Faculty of Arts and Sciences, Cyprus International University, Nicosia, North Cyprus, Mersin 10, Turkey.*
[3]*Cyprus Bee and Bee Products Research Centre, Cyprus International University, Nicosia, North Cyprus, Mersin 10, Turkey.*
sundayukanwa@gmail.com*

(Received on 21st March 2023, accepted in revised form 5th July 2023)

Summary: Research in nanotechnology has progressed in the last decades, and it is purposeful to explore the applications of biocompatible nanoparticles in general and their anticancer attribute specifically. This study is aimed at examining the cytotoxic effects of biocompatible Northern Cyprus propolis extract of iron oxide nanoparticles (*PE*-Fe_2O_3-NPs) on MDA-MB-231 epithelial human breast cancer cell line, in vitro. Propolis extract were used to obtain *PE*-Fe_2O_3-NPs and further characterized using several methods like ultraviolet-visible spectroscopy, Fourier-transform infrared spectroscopy, scanning electronic microscopy and X-ray diffraction analysis. The *PE*-Fe_2O_3-NPs has a distinctive Surface Plasmon Resonance band at 350 nm. The prepared *PE*-Fe_2O_3-NPs had a size of 108 nm by diameter with a zeta potential of +33.9 mV which indicates a good stability of the nanoparticles' while the size of Fe_2O_3-NPs was 89.40 nm by diameter. Antibacterial result showed that Fe_2O_3-NPs has highest Minimum Inhibitory Concentration and Minimum Bactericidal Concentration as compared to *PE*-Fe_2O_3-NPs with different concentration of propolis extract as regards the tested microorganisms. This indicates that *PE*-Fe_2O_3-NPs possesses a more effective threat to eliminating pathogenic bacteria at lesser dosages, be it Gram-ve or Gram+ve. *PE*-Fe_2O_3-NPs effectively halted the spread of MDA-MB-231 cancer cell lines and thus, prove to be commendable for anticancer biomedical uses.

Keywords: Propolis, Iron oxide, Nanoparticles, Anticancer, Antibacterial.

Introduction

The woman breast cancer is considered the second highest diagnosed cancer worldwide. A global estimation of over 2.09 million women were diagnosed in 2018 of this disease and thus resulted in about 627,000 deaths universally [1]. In all new cases of diagnosed cancer in women, 29 percent were breast cancer [2]. Modern advancements medicine considers breast cancer to be a heterogeneous versatile illness with a range of factual and mutational alterations widely of different molecular subtypes having specific clinical importance. Breast cancer treatment and management can be achieved in most cases through surgery, hormone therapies, and radiotherapy and adjuvant chemotherapy [3]. Nanoparticles are tiny particles having varying sizes ranging from 1-100nm [4].

The technology or science by which these nanoparticles are produced is known as 'Nanotechnology'. Nanoparticles are produced in different sizes and shapes and chemical composition. Iron oxide nanoparticle has many significant usages in treatments like in medicine transport, cancer treatment, hyperthermia, targeted treatment and magnetic resonance imaging [5]. The expanded or broadened study on iron oxide nanoparticle is due the following properties; non-toxic, non-immunogenic, biocompatible and biodegradability of this metal oxide.

The development of metal nanoparticles has been well studied for their anticancer potential [6]. Metal nanoparticles has in recent times been the center of attraction for researchers. Metal nanoparticles are easily synthesized, because they are chemically stable under biological circumstances, that is; they are non-toxic and biocompatible [6, 7].

Fe_2O_3 nanoparticles is fundamentally designed for various biomedical purposes, for

*To whom all correspondence should be addressed.

instance; they have been used as antimicrobial agents, cellular labelling and separation, targeted drug delivery and tissue repair [6, 8-10]. So as to escape aggregation of Fe_2O_3 nanoparticles, improve their biocompatibility, biological application and firmness, the situation is conceivable toward functionalizing these biomolecules. Certain biological and naturally occurring plants such as propolis have gained a reputation as exceptional materials as well as demonstrate medicinal significance in the past.

Propolis is a product of honey bee gotten from different plant gums and mixture of complex resin that is rich with saliva as well as enzyme secretion [11]. Propolis composition depends on different bees and the plant resin they produce, the substances they synthesis as well as the enzyme they secret. Propolis have been utilized in the past traditionally to treat many illnesses. It has biological characteristics like antitumor, fungicidal, anti-inflammatory, antioxidant, antiviral agent and antibacterial effects [12-14]. Propolis is made up of over 108 bioactive compounds, many has antioxidant characteristics like phenols (Polyphenol and Flavonoid) [15]. This research therefore intents to synthesize, study as well as assess the cytotoxicity of Northern Cyprus Propolis extract Fe_2O_3 nanoparticles (*PE*-Fe_2O_3-NPs) delivery system on breast cancer cell. Furthermore, this investigation offers evidence on production by means of novel approach to acquire targeted delivery systems with stable and effective structures.

Experimental

Collection of propolis

Propolis were collected from the various sections of Cyprus (North West, North, North East, Central Cyprus and South West,). The sites of sampling were revealed on the map in Fig 1. Propolis ploys were positioned into the hives at designated apiaries in the period of 7 days. The collected Samples were kept at −20 °C pending processing.

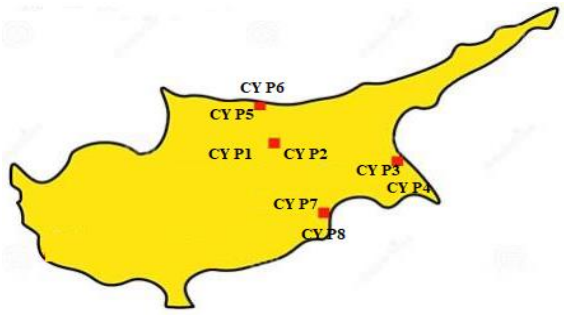

Fig. 1: Sampling Sites of Propolis CY P indicates Cyprus Propolis.

This collection was done in 4 metropolises from 8 localities in Cyprus. The obtained samples from Nicosia (CY P1, CY P2), Magusa (CY P3, CY P4), Girne (CY P5, CY P6), Morphou (CY P7, CY P8), were near the forest, which largely has gymnosperm plants such as *Pinus* spp. and *Juniperus* spp.

Preparation of propolis extracts

55 g of powdered fresh propolis was liquefied in 1 L of solvent mixture encompassing distilled water and ethanol in the proportion (3:7) and placed in an incubator at room temperature (25 °C) in an open shaker for about a week in the dark. The liquefied brown colored solution was strained with the use of Whatman number 1 filter paper and the remains was subsequently removed. The filtrate was vaporized with the aid of rotary vacuum evaporator. The ensuing brown shaded sticky affluence was utilized as ethanolic extract of propolis (EEP).

Green Synthesis of Propolis Iron Oxide Nanoparticles (PE-Fe_2O_3-NPs)

Briefly, 0.54 g of ferrous chloride tetra hydrate and 1.09 g of Ferric chloride hexahydrate and (2/1 molar ratio) was liquefied in 100 mL of sterilized deionized distilled water in a 250 mL beaker and heated at 85°C with the use of magnetic stirrer and in atmospheric pressure for 1o minutes, then 5 mL of the aqueous solution of propolis extract was mixed with the above solution drop-wisely with an observed transformation in yellowish color of the mixture to reddish brown color. After 5 min, 25 mL of 1 M NaOH (0.8 gm) was thawed in sterilized deionized distilled water in a beaker 50 mL and introduced to the mixture at the rate of 3 mL per minute to allow the precipitations of the magnetite equivalently. Starting from the initial addition of NaOH, the reddish-brown color of the mixture transformed to brownish black suspended particles. The mixture was permitted to drop temperature to 25°C and the iron oxide nanoparticles was gotten by decantation after the dilution with sterilized distilled water and centrifugation for the removal of heavy biomaterials of the extract. The nanoparticles were cleansed by dissolving in sterilized distilled water and centrifuged three times.

$$2Fe^{3+} + Fe^{2+} + \text{PE} + H_2O \rightarrow [(2Fe^{3+}: Fe^{2+}) / \text{PE} \quad (1)$$

$$[(2Fe^{3+}: Fe^{2+})/\text{PE} + O_2 \rightarrow \text{Iron oxide nanoparticle / PE} \quad (2)$$

Characterization technique

Ultraviolet-visible spectrophotometry surface plasmon resonance (SPR) was recorded at wavelengths of 200 to 1000 nm. Fe_2O_3-NPs and *PE*-Fe_2O_3-NPs possesses crystal-like arrangements under X-ray diffractometer when evaluated. Using Zetasizer system (Malvern ZS Nano ZS90) having Malvern Software, polydispersity property as well as the zeta size of Fe_2O_3-NPs and *PE*-Fe_2O_3-NPs were characterized. Scanning electron microscope of 14kV voltage speed was utilized to evaluate the surface morphology of both Fe_2O_3-NPs and *PE*-Fe_2O_3-NPs. FTIR spectroscopic examination of samples were obtained when KBr residue and pellets were blended. Subsequent drying, demonstrated as a spectrum using a spectrophotometer at a wavelength of 400 cm−1 and 4000 cm−1.

Antimicrobial activity evaluation

For the investigation of antimicrobial activity, minimum inhibitory concentration and minimum bactericidal concentration was evaluated with the use of two gram-positive (*Bacillus subtillis* and *Streptococcus pyogenes*) and two gram-negative (*Pseudomonas aeruginosa*, and *Escherichia coli*) bacterium, Mixture of diverse concentrations of the prepared nanoparticles and the same volume of sterilized nutrient broth were prepared and 20 µL of bacteria (corresponding to 0.5 McFarland) was introduced into respective test-tubes. The tubes were incubated for 24hrs, samples in respective tubes were introduced into nutrient agar plates and allowed to grow. Minimum inhibitory concentration was calculated and demonstrated minimal inhibition zone, which showed about ten colonies. On the other hand, minimum bactericidal concentration demonstrated lowest concentration without any colony, radial diffusion assay was primarily utilized when investigating this. Carrying out this procedure, bacterium solution of 1 mL was incorporated with Mueller Hinton Agar. After 24hr, blank disk drenched with the sample and incubated were placed on the medium. The control experiment was a penicillin disk however, 24h later, area of inhibition was measured [25].

Evaluation of cytotoxicity PE-Fe_2O_3-NPs

The MDA-MB 231 epithelial human breast cancer cell lines were gotten from the cell bank of the Biotechnology Research Centre of CIU. Cell culture was formed at 80–90% confluence in a culture plate with the DMEM medium comprising penicillin (100 U/mL), streptomycin (100 µg/mL) and fetal bovine serum (FBS; 10%) at 37°C. Then, the effect of *PE*-Fe_2O_3NPs at diverse concentrations (5, 10, 15, 25, 50, 75, 100 µg/mL) on MDA-MB 231 cell viability was examined for 24 h. MTT (Sigma, USA) stain was employed to evaluate the cytotoxicity of the prepared *PE*-Fe2O3NPs on MDA-MB 231. Initially, the cell suspension was made from standard cells, and 200 µL of this suspension was introduced to each well from 96 house plates. Ten thousand cells were fixed in cell culture plates and treated with *PE*-Fe_2O_3-NPs concentrations of 5, 10, 15, 25, 50, 75, 100 µg/mL. After 24 h, 20 µL of MTT dye (with a final concentration of 5 mg/ml) was introduced to the wells and placed in incubation for 5 h at 37° C with 5% CO2. The top-layer solution was eliminated, and formazan crystals were liquified in 150 µL of DMSO. Furthermore, at 570 nm, the wells were checked for absorbance by means of an ELISA reader (Epoch, Biotek USA). Formulae for cell viability calculation below:

$$Cell\ viability\ (100\%) = \frac{sample\ absorption}{control\ absorption} \times 100 \qquad (3)$$

Statistical analysis

In any case, every single trial was carried out in thrice. Prism GraphPad as well as the Origin Pro 9 software programs stayed utilized in evaluating the entire data. One-way analysis of variance was used to investigate the data and the Duncan post-hoc test (P-value < 0.05).

Results and Discussion

The synthesize and characterization of PE-Fe_2O_3NPs

The size of the prepared sample and their respective Zeta potential analysis were done to evaluate the size as well as stability of the nanoparticles in colloidal suspension. *PE*-Fe_2O_3-NPs zeta sizer result showed that the particles had a 108.43 ± 5.11 nm size as indicated in Fig 2b, while the particles for Fe_2O_3NPs were 89.40 ± 5.11 nm as showed in Fig 2c, while showing a Polydispersity Index value of 0.26 ± 0.10 which is an indication of good nanoparticle size. Fig 2a; demonstrates Zeta potential value of the biosynthesized *PE*- Fe_2O_3-NPs. Result revealed zeta potential value to be +33.9 mV. This high value is an indication that the synthesized NPs are very stable in suspension. It also means that the NPs possess the tendency to eject one another as well as inhibit accumulation of NPs. The deep-rooted stability of NPs in the solution are as a result of their high electrostatic repulsion force (ERF). The cells attract this

nanoparticle because of their differences in charges. Though, this procedure depends on cell type. The result we got validates those of other scholars [16].

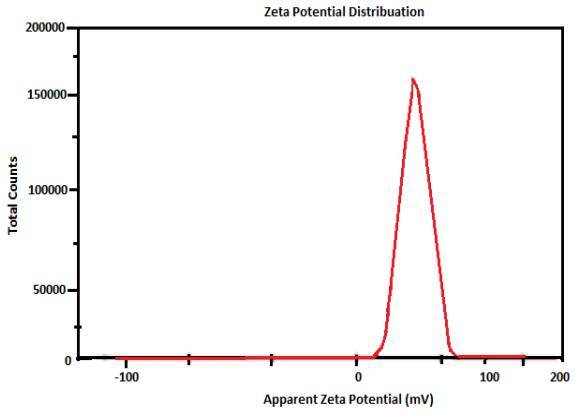

(a)

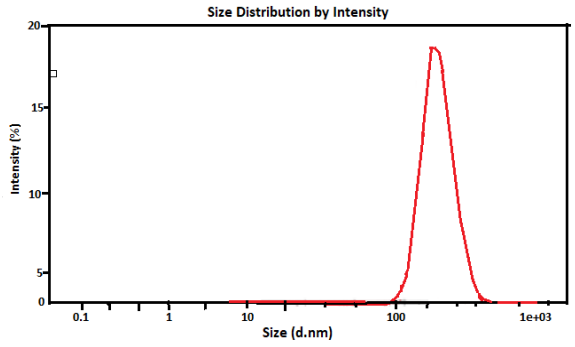

(b)

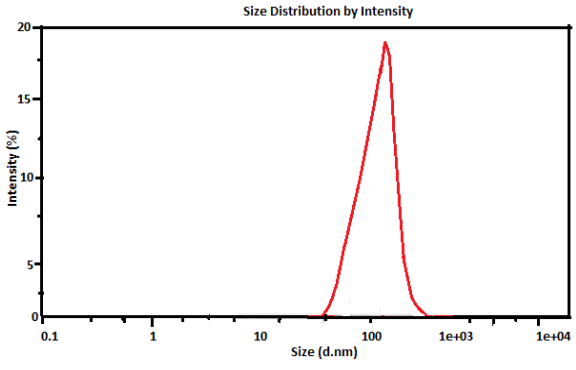

(c)

Fig. 2: (a) *PE*- Fe_2O_3-NPs zeta potential; (b) *PE*-Fe_2O_3-NPs Zeta Size; (c). Fe_2O_3NPs Zeta size.

The Fig 2 demonstrates the spectrum obtained from an ultraviolet-visible spectrophotometer for *PE*-Fe_2O_3-NPs. The result showed spectrum wavelength range between 200-1000 nm. Fe^+ was reduced to FeO at broad peak 350 nm and thus showed the formation of *PE-Fe₂O₃-NPs*. The distinctive peak seen was owing to change in color as well as formation of NPs because of the Surface Plasmon Resonance (SPR) excitation state. Makarov et al., [17] reported something similar; *PE*-Fe_2O_3-NPs demonstrated this distinctive peak at range 350-400 nm. Peak widening was as a result of a number of influences, which include shape, particle size and polydispersity of nanoparticle [18].

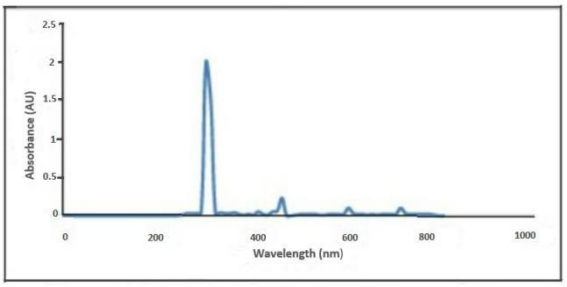

Fig. 3: UV-VIS Spectrophotometry analysis of *PE*-Fe_2O_3-NPs.

The FTIR spectra of ethanolic extract of Cyprus propolis, PE- Fe_2O_3-NPs (Fig 4) demonstrates existence of the efficient functional groups as well as structural alterations in course of the procedure. The hydroxyl groups (-OH) in propolis extract spectrum has a broadband at 3596 cm−1 that also looked at 3382 cm−1 in *PE*-Fe_2O_3-NPs [19, 20] (Fig 4a and 4b). The disappearance of the bands in the PE- Fe_2O_3-NPs spectrum which is clearly seen at bands 1622 and 1398 cm−1 in the ethanolic propolis extract as well as PE-Fe_2O_3NPs bands is as a result of the presence of carboxylate. There is an absorption band at 1622 and 1076 cm−1 which is accredited to the shuddering of C=O and C–O of the carboxylic acid is as a result of the existence of biological composites from propolis extract in *PE*- Fe_2O_3-NPs (4b). Peaks in Fe_2O_3-NPs were clearly visible at 517, 621, 1020, 1612, and 3435 cm-1 (Fig 4c). The vibrational basic broadening of the metal-oxygen bond vibrations (Fe-O) caused two clearly separate peaks to arise at 517 cm-1 and 621 cm-1, indicating that the generated NPs were iron oxide [21,22]. Owing to the irregular stretching of Fe-O, a faintly slighter peak at 1020 cm-1 was present. The use of NaOH in the production of the Fe_2O_3-NPs may be the cause of the absorption peaks that occurred at 1612 cm-1 and 3495 cm-1, which indicate the flexible vibration of engrossed water and surface hydroxyl (-OH) groups [23].

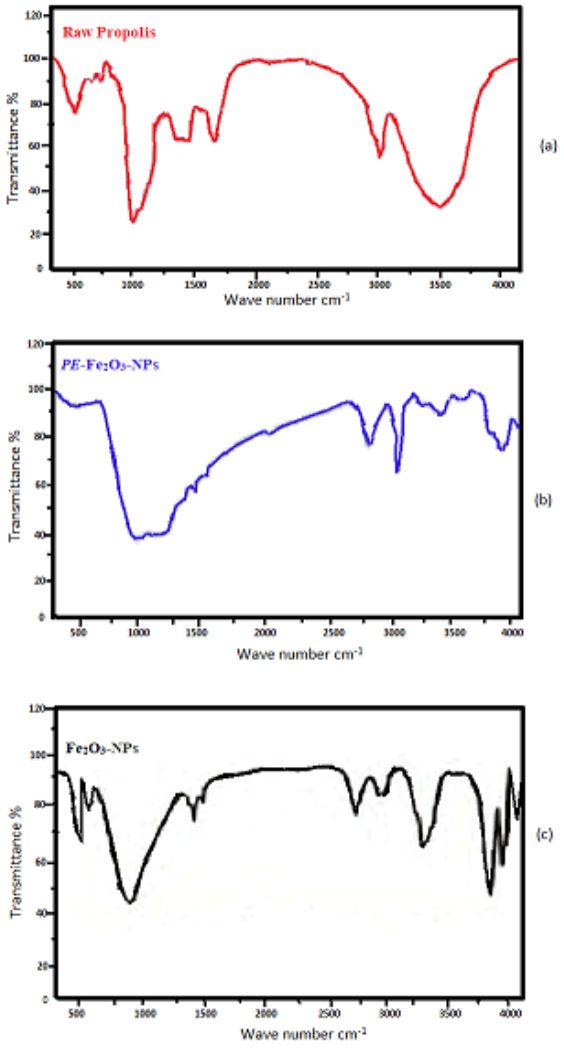

Fig. 4: The FTIR analysis of both (a) ethanolic extract of propolis; (b) *PE*- Fe_2O_3-NPs and (c) Fe_2O_3-NPs.

The Fe_2O_3-NPs X-ray diffraction spectrum that were created utilizing the ethanol extract of propolis is shown in Fig 5a. This spectrum has a wavelength of 1.54 nm as well as a recorded speed rate of one degree per minute in the 2θ/θ array of 20 to 80°. The crystal phase of *PE*- Fe_2O_3-NPs is depicted by the indexed diffraction peaks in the picture. The average size D of crystallite confirmed at 36.4 nm.

$$d = \frac{k\lambda}{\beta cos\theta} \qquad (5)$$

where d represents *PE*- Fe_2O_3-NPs average crystalline size, k has a value of 0.9-1 and X-ray wavelength of 1.54 nm, b stands for broadening line in radius while Bragg angle is h. The supposed crystalline size of *PE*- Fe_2O_3-NPs from the equation was under 23 nm, thereby giving the highest peak for *PE*- Fe_2O_3-NPs at 36.4 nm average size. At the time of synthesis, pH of the medium was raised 10.8 owing to addition of NaOH to the solution of Fe salt and Propolis extract. Fig 5B shows the XRD result of the nanoparticles. The results of the XRD examination are in agreement with the tetragonal structure of α- Fe_2O_3 nanoparticles [24]. Debye Scherrer equation was used to calculate the crystalline size average D thus demonstrated the relationship between the crystalline size as well as the *PE*- Fe_2O_3-NPs. The results of the diffraction in this study are in agreement with the recorded data of the Joint Committee on Powder Diffraction Standards (JCPDS) card number 33-0664. A minor peak of γ-Fe_2O_3 is seen at 2θ of 30.7°. The diffraction peak's broadening line significantly shows that the Fe_2O_3-NPs sample size is of the nm scale.

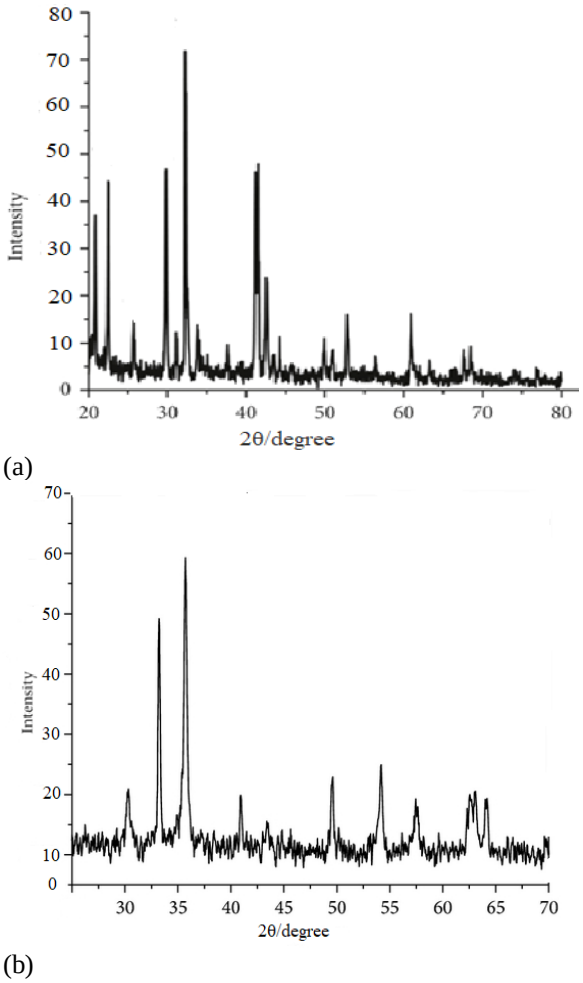

Fig. 5: The XRD analysis of (a) *PE*- Fe_2O_3-NPs & (b) Fe_2O_3NPs.

Scanning electron microscopic analysis was demonstrated to determine the morphology of the synthesized *PE*- Fe_2O_3-NPs in Fig 6 in which a varied size was observed with nanoparticles have a tendency to agglomerate but propolis extract component around the nanoparticles is inhibiting from aggregation. The image also showed that the fabricated *PE*- Fe_2O_3-NPs are spherical in shape. Quite a few authors found that this variation could occur as a result of a mixture of compounds present in the propolis extract with diverse reducing properties and stabilization [26]. The nanoparticles seem to be agglomerated as well as spherical. The electrostatic interaction between the surface layers of the nanoparticles may have caused the agglomeration of PE-Fe_2O_3NPs that was seen [27]. Furthermore, the propensity of nanoparticles to amass in suspension is as a result of its high surface area [28].

Antimicrobial activity

Antibacterial experimental results stand presented in table 1. Giving the results, the synthesized nanoparticles exhibited significant antibacterial efficacy against both gram+ve and gram-ve bacteria. Results indicated that at 7.5% propolis extract nanoparticles, Minimum Inhibition Concentration as well as Minimum Bactericidal Concentration showed substantial statistical variance and thus, becomes statistically inconsequential even when dosage were further increased. Consequently, the *PE*- Fe_2O_3-NPs with 7.5% dosage level demonstrated the best antibacterial activity. The minimum inhibition concentration for functionalized *PE*- Fe_2O_3-NPs on Bacillius subtillis, Staph. aureus, and E. coli were 0.46, 0.39, and 0.19 mg mL-1, with the consistent value of MIC of 0.15, 0.113, and 0.098 mg mL-1, subsequently. Based on earlier reports, PE and Fe_2O_3-NPs demonstrated effective antibacterial actions towards numerous pathogens [29-31]. The main mechanisms underlying the antibacterial action of iron oxide nanoparticles are interference of cell membrane caused by dipole-dipole, hydrogen, and hydrophobic collaboration with the membrane of bacteria as well as formation of ROS [32,33].

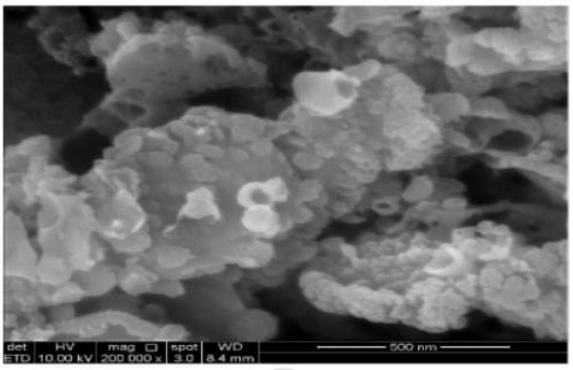

Fig. 6: Scanning Electron Microscopy Image showing PE-Fe_2O_3NPs.

The results of the Recommended Dietary Allowance procedure validated Minimum Inhibitory Concentration as well as Minimum Bactericidal Concentration demonstrated in Table 2, increment in the dosage ratio of PE- Fe_2O_3-NPs *up* to 7.5% brought about an increase in inhibition growth which became insignificant as the percentage of propolis extract increases in the nanoparticles. Therefore, the synergistic effect of the nanoparticles prepared with propolis extract can be attributed to the improvement in antibacterial activity laterally because of the increase in the proportion of green iron oxide nanoparticles [25]. Iron oxide nanoparticles having 7.5% propolis extract according to the result, recorded optimal antimicrobial action.

Table-1: MIC and MBC evaluation of pure and green synthesized nanoparticles on *Bacillius Subtillis, Staphylococcus aureus, Escherichia coli, and Pseudomonas aeruginosa.*

.		0	0.5	1	2	2.5	5	7.5	8.5	10
Bacillius subtillis	**MIC (mg mL−1)**	**1**	**1**	**0.85**	**0.22**	**0.21**	**0.18**	**0.15**	**0.15**	**0.155**
	MBC (mg mL−1)	**2**	**2**	**1.55**	**0.5**	**0.5**	**0.55**	**0.46**	**0.47**	**0.46**
Staphylococcus aureus	**MIC (mg mL−1)**	**1**	**0.45**	**0.45**	**0.25**	**0.125**	**0.12**	**0.113**	**0.113**	**0.112**
	MBC (mg mL−1)	**1.75**	**1.85**	**0.65**	**0.6**	**0.48**	**0.455**	**0.39**	**0.39**	**0.385**
Escherichia coli	**MIC (mg mL−1)**	**0.5**	**0.26**	**0.285**	**0.125**	**0.124**	**0.125**	**0.098**	**0.09**	**0.098**
	MBC (mg mL−1)	**1**	**0.55**	**0.55**	**0.25**	**0.22**	**0.22**	**0.19**	**0.185**	**0.185**
Pseudomonas aeruginosa	**MIC (mg mL−1)**	**1**	**0.55**	**0.55**	**0.25**	**0.22**	**0.22**	**0.19**	**0.19**	**0.19**
	MBC (mg mL−1)	**1.75**	**1.05**	**1.06**	**0.55**	**0.5**	**0.5**	**0.40**	**0.40**	**0.39**

Table-2: Inhibition zones of bacteria after treatment.

Bacterium	**Inhibition zone (mm)**								
	0	**0.5**	**1**	**2**	**2.5**	**5**	**7.5**	**8.5**	**10**
Bacillius subtillis	**18**	**19**	**19**	**35**	**36.5**	**38**	**40**	**40**	**40**
Staphylococcus aureus	**17**	**18**	**19**	**34**	**34**	**35**	**35**	**35**	**35**
Escherichia coli	**14**	**14**	**15**	**20**	**24**	**27**	**28**	**28**	**28**
Pseudomonas aeruginosa	**14**	**14**	**16**	**17**	**17**	**272**	**27**	**27**	**27**

Cytotoxicity test

The results detail the action of green-synthesized PE- Fe_2O_3-NPs at stable room temperature and neutral pH. This study further examined the toxicity of Fe2O3NPs prepared using Propolis extract against human breast MDA-MB 231 cells at 5, 10, 15, 25, 50, 75, 100 µg/mL doses through the MTT colorimetric technique. Additionally, cell viability ratio was evaluated 24 h later. MDA-MB 231 epithelial human breast cancer cell lines were treated with varying dosages of *PE*-Fe2O3NPs and thus, were dose-dependent thereby demonstrating significant cytotoxicity effects. Certainly, efficient cytotoxic properties were observed at 75 µg/mL as well as 100 µg/ml dosages, and quantity of inhibitory concentration (IC50) was 17.21 µg/mL (Fig 7). Cytotoxicity result recorded, were in accordance with that of Mathew et al. [34] and Ogbonna and Kavaz [35] who also reported dose-dependent significant effects of treatment on the cells. In other studies, [36-38] all reported the cytotoxicity effects of green synthesized nanoparticles. The common explanation in all of their studies is that increase in the concentration of the extract used brought bought about a significant increment in the cytotoxicity effect until an equilibrium was reached.

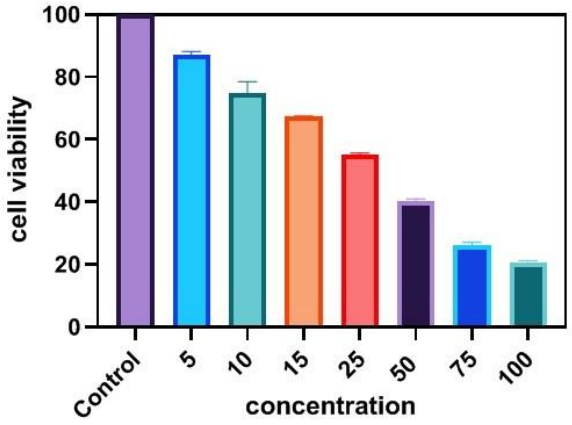

Fig. 7: The results of the survival percentage compared to control samples of MTT assay in MDA-MB 231 epithelial human breast cell lines treated by PE-Fe_2O_3NPs after 24 h.

Conclusions

Conclusively, green-synthesized nanoparticles were prepared using propolis. The obtained particles were characterized with the use of UV-Vis, SEM, XRD and FTIR. The average size for *PE*-Fe_2O_3NPs were around 108.43 ± 5.11 nm while the particles for Fe_2O_3NPs were 89.40 ± 5.11 nm. Distinctive SPR bands for Fe2O3NPs were between 350 and 400nm as described previously, and a noticeable single band proposes that the nano-morphology of the particles may be sphere-shaped. The spectrum of the FTIR of *PE*- Fe_2O_3NPs show more organic compound peaks than that of Fe_2O_3NPs as expected due to the presence of propolis extract. The antimicrobial evaluation trial in this investigation demonstrated that *PE*- Fe_2O_3NPs were more active against microorganisms than the Fe_2O_3NPs. Besides, this work weighed the effectiveness of *PE*- Fe_2O_3NPs and its cytotoxic activity on human cancer cell line for 24 hrs. Nevertheless, in the *PE*- Fe_2O_3NPs -treated plates, a significant reduction in the cell number observed as the concentration of the treatment increases. The concentration may have prejudiced the reaction of the MDA-MB-231 cells to the *PE*-Fe_2O_3NPs, consequential to the variances in the number of dead and active cells after the treatment. It is sufficient to conclude that the relationship was very directly relational. The *PE*- Fe_2O_3NPs competently halted the proliferation of MDA-MB-231 cancer cells and could substantiate to be commendable a candidate for biomedical anticancer applications.

*Author Contributions***:** Formal analysis, S.U., and E.O.; investigation, S.U., and E.O.; methodology S.U., and E.O.; supervision, E.O.; validation, S.U., and E.O. All authors have read and agreed to the published version of the manuscript.

Acknowledgments

The authors wish to appreciate the efforts and help of the researchers working in the Biotechnology Research Centre (BRC) of the University.

References

1. World Health Organization. Cancer. Available online: http://www.who.int/news-room/fact-sheets/detail/ cancer (accessed on 16 January 2023)
2. K. D. Miller, R. L. Siegel, C. C. Lin, A. B. Mariotto, J. L. Kramer, J. H. Rowland, K. D. Stein, R. Alteri, and A. Jemal, "Cancer statistics, 2016," CA*: A Cancer J.*, 66, 271 (2016).
3. H.-H. Chou, W.-L. Kuo, C.-C. Yu, H.-P. Tsai, S.-C. Shen, C.-H. Chu, M.-C. Yu, Y.-F. Lo, M. A. Dabora, H.-K. Chang, Y.-C. Lin, S.-H. Ueng, and S.-C. Chen, "Impact of age on pathological complete response and locoregional recurrence in locally advanced breast cancer after neoadjuvant chemotherapy, *Biomed. J.*, 42, 66

(2019).
4. M. Shah, D. Fawcett, S. Sharma, S. Tripathy, and G. Poinern, Green Synthesis of Metallic Nanoparticles via Biological Entities., *Materials.*, **8**, 7278 (2015).
5. J. Kudr, Y. Haddad, L. Richtera, Z. Heger, M. Cernak, V. Adam, and O. Zitka, Magnetic Nanoparticles: From Design and Synthesis to Real World Applications, *Nanomaterials.*, **7**, 243, (2017).
6. S. El-Guendouz, S. Aazza, B. Lyoussi, M. D. Antunes, M. L. Faleiro, and M. G. Miguel, Anti-acetylcholinesterase, antidiabetic, anti-inflammatory, antityrosinase and antixanthine oxidase activities of Moroccan propolis, *Int. J. Food Sci. Technol.*, **51**, 1762 (2016).
7. S. El-Guendouz, B. Lyoussi, J. P. Lourenço, A. M. Rosa da Costa, M. G. Miguel, C. Barrocas Dias, A. Manhita, L. Jordao, I. Nogueira, and M. L. Faleiro Magnetite nanoparticles functionalized with propolis against methicillin resistant strains of Staphylococcus aureus., *J Taiwan Inst Chem Eng.*, **102**, 25 (2019).
8. I. Liakos, A. Grumezescu, and A. Holban, Magnetite Nanostructures as Novel Strategies for Anti-Infectious Therapy, *Molecules.*, **19**, 12710 (2014).
9. X. Jing, L. Yang, X. Duan, B. Xie, W. Chen, Z. Li, and H. Tan, In vivo MR imaging tracking of magnetic iron oxide nanoparticle labeled, engineered, autologous bone marrow mesenchymal stem cells following intra-articular injection, *Jt.*, **75**, 432 (2008).
10. A. S. Arbab, L. A. Bashaw, B. R. Miller, E. K. Jordan, B. K. Lewis, H. Kalish, and J. A. Frank, Characterization of Biophysical and Metabolic Properties of Cells Labeled with Superparamagnetic Iron Oxide Nanoparticles and Transfection Agent for Cellular MR Imaging, *Radiology.*, **229**, 838 (2003).
11. M. Hasan, M. Kulsum, M. Ullah, M. M. Hossain, and M. E. Mahmud, Genetic diversity of some chili (Capsicum annuum L.) Genotypes, *IJARIT*., **4**, 32 (2014).
12. A. M. Alqarni, K. Niwasabutra, M. Sahlan, H. Fearnley, J. Fearnley, V. A. Ferro, and D. G. Watson, Propolis Exerts an Anti-Inflammatory Effect on PMA-Differentiated THP-1 Cells via Inhibition of Purine Nucleoside Phosphorylase,*Metabolite*., 9, (2019).
13. S. Farida, M. Sahlan, E. Rohmatin, and R. Adawiyah, The beneficial effect of Indonesian propolis wax from Tetragonula sp. as a therapy in limited vaginal candidiasis patients, *Saudi J Biol Sci*., **27**, 142 (2020).
14. M. Sahlan, K. F. Mahira, D. K. Pratami, R. Rizal, M. J. Ansari, K. M. Al-Anazi, and M. A. Farah, The cytotoxic and anti-inflammatory potential of Tetragonula sapiens propolis from Sulawesi on raw 264.7 cell lines, *J King Saud Univ Sci*., **33,** 101314 (2021).
15. N. Segueni, A. Zellagui, F. Moussaoui, M. Lahouel, and S. Rhouati, Flavonoids from Algerian propolis, *Arab. J. Chem.*, **9**, (2016).
16. Y. P. Yew, K. Shameli, M. Miyake, N. B. B. Ahmad Khairudin, S. E. B. Mohamad, T. Naiki, and K. X. Lee, Green biosynthesis of superparamagnetic magnetite Fe3O4 nanoparticles and biomedical applications in targeted anticancer drug delivery system: A review, *Arab. J. Chem.*, **13**, 2287 (2020).
17. V. V. Makarov, A. J. Love, O. V. Sinitsyna, S. S. Makarova, I. V. Yaminsky, M. E. Taliansky, and N. O. Kalinina, Green Nanotechnologies: Synthesis of Metal Nanoparticles Using Plants, *Acta Nat*., **6**, 35 (2014).
18. K. Rajendran, V. Karunagaran, B. Mahanty, and S. Sen, Biosynthesis of hematite nanoparticles and its cytotoxic effect on HepG2 cancer cells, *Int. J. Biol. Macromol*., **74**, 376 (2015).
19. S. Sharma, K. Singh, S. Sharma, K. Kumar, S. Chauhan, and M. S. Chauhan, Facile Growth and Characterization of α-Fe_2O_3 Nanoparticles for Photocatalytic Degradation of Methyl Orange, *J. Nanosci. Nanotechnol*., **14**, 6153 (2022).
20. S. W. Hwang, A. Umar, G. N. Dar, S. H. Kim, and R. I. Badran, Synthesis and Characterization of Iron Oxide Nanoparticles for Phenyl Hydrazine Sensor Applications, *Sensor Letters*., **12**, 97 (2014).
21. R. Y. Hong, B. Feng, L. L. Chen, G. H. Liu, H. Z. Li, Y. Zheng, and D. G. Wei, Synthesis, characterization and MRI application of dextran-coated Fe_3O_4 magnetic nanoparticles, *Biochem. Eng. J*., **42**, 290 (2008).
22. S. Bruni, F. Cariati, M. Casu, A. Lai, A. Musinu, G. Piccaluga, and S. Solinas, IR and NMR study of nanoparticle-support interactions in a Fe2O3-SiO2 nanocomposite prepared by a Sol-gel method, Nanostructured Materials., **11**, 573 (1999).
23. F. Wang, X. F. Qin, Y. F. Meng, Z. L. Guo, L. X. Yang, and Y. F. Ming, Hydrothermal synthesis and characterization of α-Fe2O3 nanoparticles, *Mater. Sci. Semicond. Process*., **16**, 802 (2013).

24. F. Buarki, H. AbuHassan, F. Al Hannan, and F. Z. Henari, Green Synthesis of Iron Oxide Nanoparticles Using Hibiscus rosa sinensis Flowers and Their Antibacterial Activity, *J. Nanotechnol*., 2022, 1 (2022).
25. M. R. Parsaeian, A. M. Haji Shabani, S. Dadfarnia, H. Zare-Zardini, H. Soltaninejad, and M. J. Forouzani-Moghaddam, Evaluating the biological activities of functionalized magnetic iron oxide nanoparticles with different concentrations of aqueous pine leaves extract, *J. Indian Chem. Soc*.**, 99,** 100707 (2022).
26. A.H. Christine, H. Sawaya, I. Barbosa, S. Cunha, and M. Marcucci, Analytical methods applied to diverse types of Brazilian propolis, *Chem. Cent. J.*, **5**, 1 (2011)
27. E. Yusefi-Tanha, S. Fallah, A. Rostamnejadi, and L. R. Pokhrel, Root System Architecture, Copper Uptake and Tissue Distribution in Soybean (Glycine max (L.) Merr.) Grown in Copper Oxide Nanoparticle (CuONP)-Amended Soil and Implications for Human Nutrition, *Plants*., **9**, 1326 (2020).
28. G. H. Bae, Y. S. Kim, J. Y. Park, M. Lee, S. K. Lee, J. C. Kim, J. G. Kim, Y. J. Shin, H. Lee, S.-Y. Kim, Y.-S. Bae, B. A. Zabel, H. S. Kim, and Y.-S. Bae, Effect of agglomeration of silver nanoparticle on nanotoxicity depression, *Blood*.,**140**, 889 (2022).
29. E. Barzan, S. Mehrabian, and S. Irian, Antimicrobial and Genotoxicity Effects of Zero-valent Iron Nanoparticles, *Jundishapur J Microbiol*., **7**, (2014).
30. M. L. Vică, M. Glevitzky, D. M. Tit, T. Behl, R. C. Heghedűş-Mîndru, D. C. Zaha, F. Ursu, M. Popa, I. Glevitzky, and S. Bungău, The antimicrobial activity of honey and propolis extracts from the central region of Romania, *Food Biosci*., **41**, 101014 (2021).
31. T. N. Afata, R. Nemo, N. Ishete, G. T. Tucho, and A. Dekebo, Phytochemical investigation, physicochemical characterization, and antimicrobial activities of Ethiopian propolis, *Arab. J. Chem.*, **15**, 103931 (2022).
32. P. N. V. K. Pallela, L. K. Ruddaraju, S. C. Veerla, R. Matangi, P. Kollu, S. Ummey, and S. V. N. Pammi, Synergetic antibacterial potential, dye degrading capability and biocompatibility of Asperagus racemosus root assisted ZnO nanoparticles, *Mater. Today Commun.*, **25**, 101574 (2020).
33. H. Shareef, Z. Kareem, and A. Alkaim, Evaluation of antibacterial activity of Fe_2O_3 nanoparticles against Shigella dysenteriae, *J. Pharm. Sci* **10**, 1980 (2018).
34. S. Mathew, C. P. Victório, J. Sidhi M S, and B. T. B.H, Biosynthesis of silver nanoparticle using flowers of Calotropis gigantea (L.) W.T. Aiton and activity against pathogenic bacteria, *Arab. J. Chem.*, **13**, 9139 (2020).
35. C. Ogbonna and D. Kavaz, Development of novel silver-apple pectin nanocomposite beads for antioxidant, antimicrobial and anticancer studies,Biologia., **77**, 879 (2022).
36. A. W. Alshameri. M. Owais, I. Altaf, and S. Farheen, Rumex nervous mediated green synthesis of silver nanoparticles and evaluation of its in vitro antibacterial, and cytotoxic activity. *OpenNano.*, **8**, 100084 (2022).
37. C. Singh, S.K. Anand, R. Upadhyay, N. Pandey, and R. Tilak, Green synthesis of silver nanoparticles by root extract of Premna integrifolia L. and evaluatiom of its cytotoxic and antibacterial activity. *Mater. Chem. Phys*., 127413 (2023).
38. M. Barzegar, D. Ahmadvand, Z. Sabouri, and M. Darroudi, Green sythesis of magnesium oxide nanoparticles by chitosan polymer and assessment of their photocatalytic activity and cytotoxicity influences. *Mater. Chem. Phys*., **301**, 127649 (2023).